Pressure studies on the antiferromagnetic Kondo semiconductor $Ce(Ru_{1-x}Rh_x)_2Al_{10}$ ($x = 0, 0.1$)

Hiroshi Tanida,[1] Kentaro Kitagawa,[2] Naoyuki Tateiwa,[3] Masafumi Sera,[1] and Takashi Nishioka[4]
[1]*Department of ADSM, Hiroshima University, Higashi-Hiroshima, 739-8530, Japan*
[2]*Department of Physics, University Tokyo, Tokyo, 113-0033, Japan*
[3]*Advanced Science Research Center, Japan Atomic Energy Agency, Tokai, Naka, Ibaraki 319-1195, Japan*
[4]*Graduate School of Integrates Arts and Science, Kochi University, Kochi, 780-8520, Japan*
(Received 5 January 2017; revised manuscript received 17 November 2017; published 19 December 2017)

We examined the electrical resistivity (ρ) of antiferromagnetic (AFM) Kondo semiconductors $Ce(Ru_{1-x}Rh_x)_2Al_{10}$ ($x = 0$ and 0.1) under pressure in order to obtain information on the electronic states under pressure, especially near the critical pressure (P_c) from the AFM ordered state to the paramagnetic one, where the Ce-4f electron character is a more localized state in $x = 0.1$ than in $x = 0$. From the results, nearly the same P_c was obtained; $P_c \sim 4.7$ and 4.5 GPa in $x = 0$ and 0.1, respectively. In both samples, the Kondo semiconducting increase of ρ is observed up to $P \sim 3$ GPa, above which, however, the increase disappears and a broad maximum appears at high temperatures. Below the maximum, ρ exhibits a metallic decrease with decreasing temperature down to the AFM transition temperature T_0, suggesting that the c-f hybridization gap could be not necessary to form the unusual AFM order. We also examined pressure effects on the magnetic susceptibility χ of both samples up to $P \sim 2$ GPa, and found that χ along the easy axis is strongly suppressed by pressure in both samples. In $x = 0$, the broad maximum just above T_0 shifts to high temperatures with increasing pressure. On the other hand, for $x = 0.1$, a clear cusp at T_0 remains sharp and no broad peak appears at least up to 2 GPa. Such a difference in the pressure response of χ could originate from the difference in the electronic state between $x = 0$ and 0.1.

DOI: 10.1103/PhysRevB.96.235131

I. INTRODUCTION

External pressure or chemical doping can control the strength of the hybridization effect between conduction and 4f electrons (c-f hybridization), whereby the ground state is varied from a magnetically ordered state to a nonmagnetic Fermi liquid one as seen in the Doniach's phase diagram [1,2]. Near the so-called quantum critical point (QCP) located in between, unconventional superconductivity or nontrivial electronic properties have been found, and extensively investigated in recent decades [3]. The ground state of these compounds is basically metallic. Meanwhile, the Kondo insulators/semiconductors exhibit a nonmetallic behavior where a narrow energy gap opens at the Fermi energy due to a strong c-f hybridization, and thereby no magnetic order appears at low temperatures [4].

The Kondo semiconductor CeT_2Al_{10} (T = Ru, Os) with the orthorhombic $YbFe_2Al_{10}$-type structure are unique compounds exhibiting an antiferromagnetic (AFM) order regardless of the Kondo semiconductor [5–7], and a number of unusual phenomena have been found. First, the AFM transition temperature, which is denoted by T_0, is very high for a usual Ce-based AF magnet [6], where $T_0 \sim 27$ and 29 K for T = Ru and Os, respectively. The magnetic anisotropy below T_0 is also unusual. The AFM ordered moment (m_{AF}) is parallel to the c axis despite a large uniaxial magnetic anisotropy along the a axis, where $m_{AF} \sim 0.4$ and 0.3 μ_B/Ce for T = Ru and Os, respectively [8–10]. With decreasing temperature, a hybridization gap opens at the Fermi energy at high temperatures above T_0 [11–14]. Another energy gap with an excitation peak at 20 meV develops in T = Ru and Os with decreasing temperature from the results of the optical conductivity [11,12], where the onset temperature of the appearance of the excitation peak is not T_0, but T_χ^{max} where the magnetic susceptibility shows a broad peak above T_0. Since the charge gap is observed in T = Ru and Os with the AFM ordering but not in T = Fe with a nonmagnetic ground state, a close relation between the charge instability and the AFM ordering has been reported. Such a gap structure was also reported from the results of the photoemission spectroscopy [13]. On the other hand, a dispersive spin-gap excitation with an energy gap also develops with lowering temperature not only in CeT_2Al_{10} (T = Ru and Os) but in $CeFe_2Al_{10}$ with a nonmagnetic ground state [15–18]. The upper edge of the excitation energy is 8, 11, and 14 meV for T = Ru, Os, and Fe, respectively. The energy scale is related to the c-f hybridization strength, where it is smallest in T = Ru, largest in T = Fe among CeT_2Al_{10} (T = Fe, Ru, Os) [6,12–14]. Recently, from the tunneling spectroscopy experiments, a further fine gap structure was found inside those two charge gaps in T = Ru and Os [14]. Despite numerous studies up to now, no comprehensive understanding of the unusual AFM order, especially the nature of the enormously high T_0, and the unusual magnetic anisotropy, has been achieved so far.

Those electronic properties are drastically changed by a tiny perturbation such as magnetic field, pressure, or chemical doping, indicating that the c-f hybridization effect plays a key role to form the unusual AFM order [19–30]. For instance, by a small amount of Rh doping, the Curie-Weiss behavior of the magnetic susceptibility along the a axis is strongly enhanced by the Rh doping [22–24]. Here, Rh has one more extra 4d electron than Ru. m_{AF} is varied from 0.4 $\mu_B \parallel c$ in $x = 0$ to 1.0 $\mu_B \parallel a$ in $x = 0.1$ [25]. The hybridization gap is strongly suppressed by Rh doping [26], suggesting that the c-f hybridization strength is suppressed by the doping. The spin gap excitation is also suppressed [24], but a very recent neutron scattering study on powder sample of $Ce(Ru_{1-x}Rh_x)_2Al_{10}$ with $x = 0.1$ does show the excitation of ~5 meV at 5 K [27]

compared with 8 meV observed in $CeRu_2Al_{10}$. Similar doping effects were reported in the Ir-doped $CeOs_2Al_{10}$ [28–30]. Here, Ir has one more extra 5*d* electron than Os. The spin-gap excitation is fairly suppressed by the Ir doping although the magnetic susceptibility is strongly enhanced [29]. Since the suppression of the T_0 by these chemical doping seems to be correlated with the suppression of the hybridization gap, it was proposed that the hybridization gap is necessary for the unusual AFM order with high T_0 [28].

The AFM ordered state is suppressed by pressure and disappears as in most of Ce-based AF magnets. In $CeRu_2Al_{10}$, T_0 is first enhanced up to $P \sim 2$ GPa, but suppressed at high pressures and then rapidly goes to zero at a critical pressure P_c between 3 and 4 GPa [6]. Since the semiconducting behavior of ρ remains at 3 GPa but disappears at 4 GPa, the hybridization gap above T_0 could be essential for the unusual AFM order. However, due to the lack of detailed measurements near P_c, it is not clear whether the Kondo semiconducting behavior above T_0 persists until P_c. This could be essential to know the role of the hybridization gap in the unusual AFM order. On the other hand, in $CeOs_2Al_{10}$, T_0 is almost independent of pressure, and suddenly disappears at $P_c \sim 2.5$ GPa [31]. The authors in Ref. [31] proposed that at the P_c the volume fraction of the AFM state disappears. Recently, the pressure dependence of lattice parameters was examined, and no discontinuity at P_c was reported [32]. Ce valence also shows no clear change at P_c [33], suggesting that the origin of P_c could be neither a structural nor a valence transition. Thus the origin of P_c as well as the role of the hybridization gap for the unusual AFM order have not been settled.

In order to clarify the electronic state near P_c, we examined detailed pressure dependencies of ρ of $CeRu_2Al_{10}$ especially near P_c, and the magnetic susceptibility χ along the easy magnetization axis. We also carried out those experiments on related $Ce(Ru_{0.9}Rh_{0.1})_2Al_{10}$ for comparison in pressure responses. From the present results, we revealed $P_c \sim 4.7$ and 4.5 GPa in $x = 0$ and 0.1, respectively, which is slightly higher than that previously reported in $x = 0$ [6]. Also, we found that the Kondo semiconducting behavior of ρ above T_0 becomes weak with increasing pressure, and disappears above 3 GPa in both samples. Above 3 GPa, ρ exhibits a broad peak at high temperatures, and shows a metallic decrease with decreasing temperature, suggesting that the hybridization gap could be not necessary to form the unusual AFM order. From the results of the pressure dependence of χ for $H \parallel a$, we found that χ is strongly suppressed by pressure in both samples although T_0 is enhanced by pressure especially in $x = 0$. While pressure suppresses χ in both samples, the pressure effect on χ is qualitatively different near T_0 between $x = 0$ and 0.1. In $x = 0$, the broad peak of χ above T_0 shifts to high temperatures with increasing pressure. On the other hand, for $x = 0.1$, no broad peak was observed but a sharp cusp of χ remains up to 2 GPa. This difference suggests a qualitative difference in the electronic state between $x = 0$ and 0.1.

II. EXPERIMENTS

Single crystals of $Ce(Ru_{1-x}Rh_x)_2Al_{10}$ ($x = 0$ and 0.1) were prepared by an Al self-flux method [34]. ρ was measured by an *ac* four-probe method down to $T = 1.2$ K up to $P \sim$ 6.5 GPa. High pressures were created using an opposed-type anvil cell made of tungsten carbide and NiCrAl alloy [35]. Magnetization under pressure has been measured with a ceramic anvil cell for the SQUID magnetometer [36] up to 2 GPa. Pressure-transmitting media are glycerin and Daphne oil 7373 for ρ and χ, respectively [37]. Pressures were determined by the superconducting transition of Pb [38]. Here, T_0 is 27 and 23 K in $x = 0$ and 0.1, respectively. These are in good agreement with those in literature [6,23]. It is noted that T_0 represents the AFM transition temperature not only for $x = 0$ but also for $x = 0.1$. The temperature dependencies of ρ and χ are roughly the same as those reported previously [6,23]. In $x = 0.1$, there are two successive transitions, but we could not find them because those are very weak in ρ and χ [23].

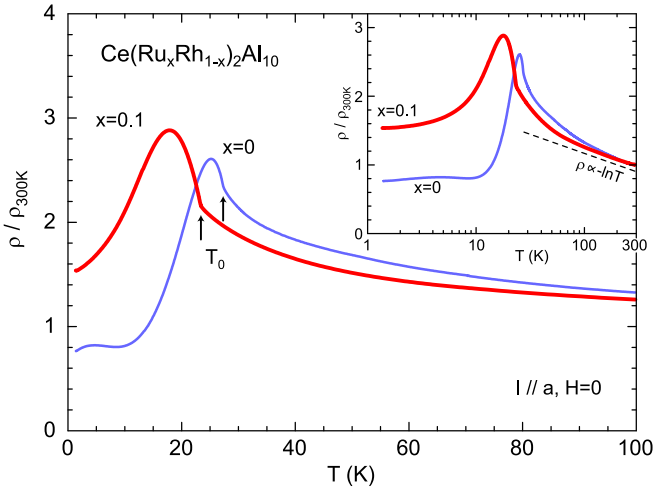

FIG. 1. Temperature dependence of the electrical resistivity (ρ) of $Ce(Ru_{1-x}Rh_x)_2Al_{10}$ ($x = 0$ and 0.1) for $I \parallel a$ at ambient pressure, where the vertical scale is normalized by ρ at $T = 300$ K. The inset represents that plotted in a logarithmic temperature scale up to 300 K. The dotted line is a guide for eyes.

III. EXPERIMENTAL RESULTS

Figure 1 shows the temperature dependence of ρ of $Ce(Ru_{1-x}Rh_x)_2Al_{10}$ ($x = 0$ and 0.1) for $I \parallel a$ at ambient pressure, where the vertical scale is normalized by ρ at $T = 300$ K. The inset gives the whole temperature dependence of ρ on a logarithmic temperature scale. ρ exhibits a dense-Kondo-like behavior at high temperatures, but undergoes a further increase exceeding the high-T logarithmic behavior, indicating an opening of the hybridization gap at low temperatures. Since the onset temperature of the increase is lower in $x = 0.1$ than in $x = 0$, the hybridization gap is suppressed by the Rh doping. At T_0, ρ exhibits a sharp upturn, followed by a broad peak located several kelvins below T_0, and shows a metallic decrease with decreasing temperature. The peak is larger for $x = 0.1$ than for $x = 0$, originating from a difference in the topology of Fermi surfaces below T_0 between $x = 0$ and 0.1 [21].

Figures 2 show the temperature dependence of ρ of $CeRu_2Al_{10}$ at various pressures up to $P \sim 5$ GPa, where $P <$ 2 GPa in Fig. 2(a), $P > 2.5$ GPa in Fig. 2(b), and the insets show those at low temperatures. With increasing pressure, a semiconducting increase appears at low temperatures and

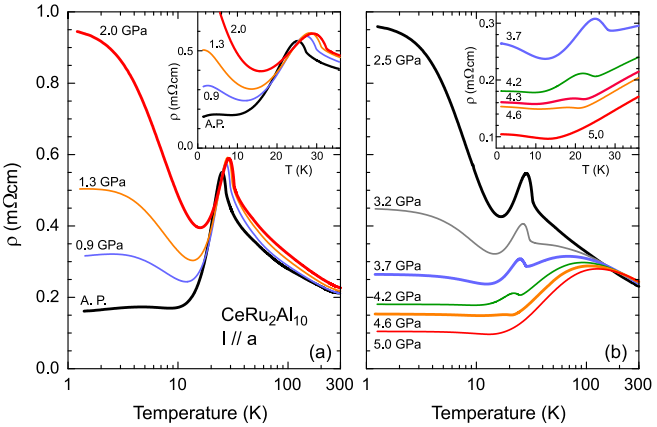

FIG. 2. Temperature dependence of the electrical resistivity of $CeRu_2Al_{10}$ for $I \parallel a$ under pressures, where (a) $P < 2$ GPa and (b) $P > 2.5$ GPa. The insets of (a) and (b) are those at low temperatures.

is enhanced up to $P \sim 2$ GPa. T_0 is also enhanced from $T_0 \sim 27$ K at the ambient pressure to 33 K at $P \sim 2$ GPa. At high pressures, the low-temperature increase of ρ is rapidly suppressed. The Kondo semiconducting increase of ρ above T_0 is also suppressed, and disappears above 3 GPa. At higher pressures, ρ exhibits a broad peak at high temperatures, followed by a metallic decrease with decreasing temperature. Nonetheless, ρ exists a clear anomaly at T_0, indicating that the AFM order appears without the Kondo semiconducting increase of ρ above T_0. Since T_0 is observed up to $P \sim 4.6$ GPa, but not at $P \sim 5.0$ GPa, P_c is located between 4.6 and 5.0 GPa, which is higher than that reported in the literature [6]. We note that all the presented data of ρ at high temperatures exhibit a weak increase with decreasing temperature. The increase could be ascribed to the magnetic scattering of the conduction electrons. A similar increase was also observed in $x = 0.1$ as will be shown below.

Figure 3 shows similar plots for $Ce(Ru_{0.9}Rh_{0.1})_2Al_{10}$ up to $P \sim 6.5$ GPa. The pressure effect on ρ is roughly the same between $x = 0$ and 0.1 except for the presence or absence

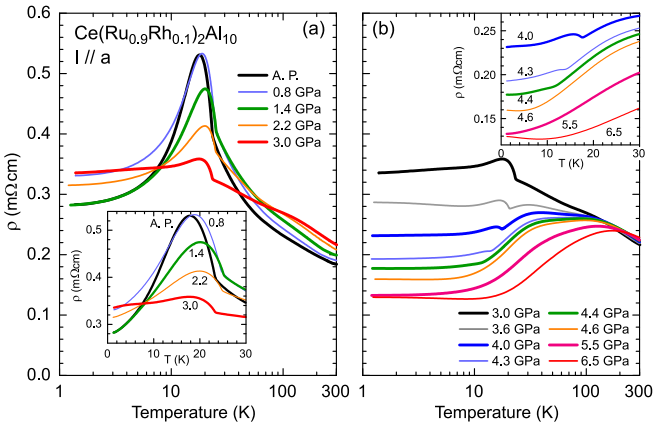

FIG. 3. Temperature dependence of the electrical resistivity of $Ce(Ru_{0.9}Rh_{0.1})_2Al_{10}$ for $I \parallel a$ at various pressures, where (a) $P < 3$ GPa and (b) $P > 3$ GPa. The insets of (a) and (b) are those at low temperatures.

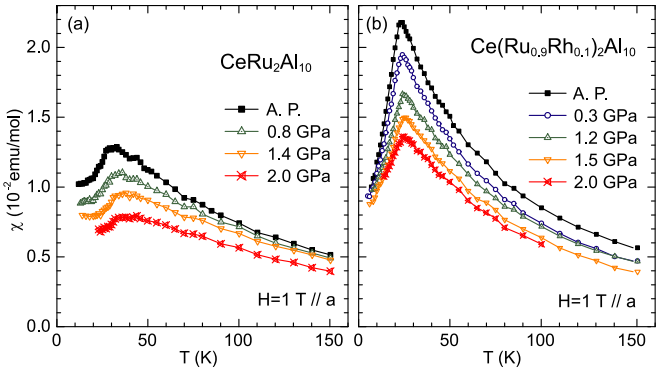

FIG. 4. Temperature dependencies of the magnetic susceptibility of $Ce(Ru_{1-x}Rh_x)_2Al_{10}$ [(a) $x = 0$ and (b) 0.1] under pressures, where $H \parallel a$.

of the semiconducting increase at low temperatures. At high pressures above $P \sim 3$ GPa, the Kondo semiconducting increase above T_0 disappears, and a broad shoulder appears at high temperatures. By further applying pressure, ρ exhibits a metallic decrease above T_0. Thus the disappearance of the Kondo semiconducting behavior above T_0 at high pressures is a common feature in both samples. Since T_0 is observed at $P \sim 4.4$ GPa but not at 4.6 GPa, we determined $P_c \sim 4.5$ GPa, which is not so much different from P_c for $x = 0$ despite many differences in electronic properties between $x = 0$ and 0.1. Above 3.6 GPa, there are two kink structures at high temperatures; one is observed at $T \sim 30$ K and another is at $T \sim 150$ K. Since the kinks shift to high temperatures with increasing pressure, those kinks are related to the c-f hybridization effect. At present, we do not know why such a two-kink-structure only appears in $Ce(Ru_{0.9}Rh_{0.1})_2Al_{10}$.

Figures 4(a) and 4(b) show the temperature dependencies of χ along the a axis (χ_a) in $Ce(Ru_{1-x}Rh_x)_2Al_{10}$ for $x = 0$ and 0.1, respectively. χ_a of both samples are suppressed by pressure. In $x = 0$, χ_a at the ambient pressure shows a broad peak at $T_\chi^{max} \sim 30$ K, and a weak decrease below $T_0 \sim 27$ K. Based on the value of T_χ^{max}, the Kondo temperature is estimated to be 90 K. With increasing pressure, both T_0 and T_χ^{max} shift to high temperatures. The increasing rates of the two characteristic temperatures are different with each other as will be shown in Fig. 5(a). On the other hand, in $x = 0.1$, χ_a shows a Curie-Weiss increase on cooling, and a sharp cusp at $T_0 \sim 23$ K, below which χ decreases steeply with decreasing temperature. This is characteristic of the AFM order with $m_{AF} \parallel a$. With increasing pressure, T_0 slightly shifts to high temperatures from $T_0 \sim 23$ to ~25 K at $P \sim 1.5$ GPa. While χ_a is suppressed, the cusp structure remains sharp within the present pressure range, suggesting that the $m_{AF} \parallel a$ state persists up to $P \sim 2.0$ GPa at least. We emphasize that, in $x = 0.1$, there is no broad peak above T_0 as is observed in $x = 0$ within the present pressure range, i.e., T_χ^{max} coincides with T_0 in $x = 0.1$.

Figure 5(a) shows the pressure dependence of T_0 of $Ce(Ru_{1-x}Rh_x)_2Al_{10}$ ($x = 0$ and 0.1). In $x = 0$, T_0 is enhanced up to $T_0 \sim 33$ K at $P \sim 2$ GPa. Above 2 GPa, T_0 is suppressed and abruptly goes to zero at $P_c \sim 4.7$ GPa. A similar pressure dependence of T_0 was reported in Ref. [6], but P_c is smaller

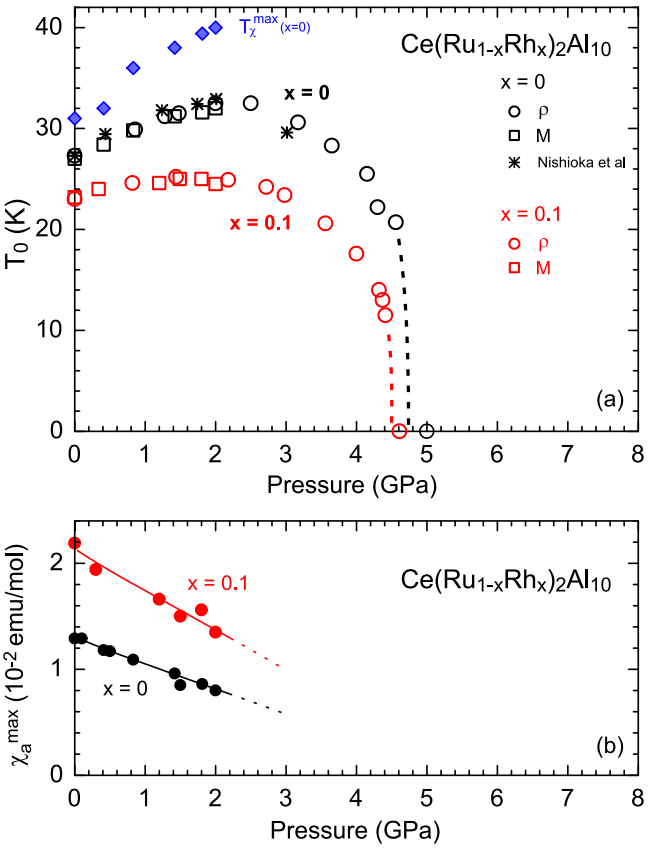

FIG. 5. (a) Pressure dependencies of the AFM transition temperature of T_0 in $Ce(Ru_{1-x}Rh_x)_2Al_{10}$ ($x = 0$ and 0.1). That of $x = 0$ reported in Ref. [6] is also shown for comparison. In (a), the temperature where the magnetic susceptibility along the a axis shows a maximum (T_χ^{max}) of the sample with $x = 0$ is also shown. (b) The maximum value of the magnetic susceptibility along the a axis (χ_a^{max}) plotted as a function of pressure for $x = 0$ and 0.1.

than that in the present study. Such a discrepancy in P_c could originate from the difference in the pressure calibration between the present and the previous study. Meanwhile, in $x = 0.1$, T_0 is only slightly enhanced up to 25 K at $P \sim 2$ GPa from 23 K at ambient pressure. At high pressures, T_0 is suppressed and suddenly disappears at $P_c \sim 4.5$ GPa as in $x = 0$. We note that T_0 is still high just below P_c; $T_0 \sim 20$ K at $P \sim 4.6$ GPa in $x = 0$, and $T_0 \sim 10$ K at $P \sim 4.4$ GPa in $x = 0.1$. In this figure, the pressure dependence of T_χ^{max} of $x = 0$ is also shown. T_χ^{max} increases gradually with increasing pressure. On the other hand, for $x = 0.1$, T_χ^{max} coincides with T_0 within the present pressure range. Figure 5(b) shows the pressure dependence of maximum values of χ_a (χ_a^{max}) of both samples as a function of pressure. χ_a^{max} is almost linearly suppressed by pressure. At $P \sim 2$ GPa, χ_a^{max} becomes a half of that at ambient pressure. Such a large suppression of χ_a^{max} contrasts with the pressure dependence of T_0, especially for the large enhancement of T_0 in $x = 0$. Here, the pressure dependence of χ_a^{max} in $x = 0$ is somewhat different from that previously reported [34]; the suppression rate is faster in the previous result than in the present one. This is possibly due to a difference in the magnetic field strength; $H = 1$ T in the present study but $H = 14.5$ T in the past one. In any case, it is evident that χ_a is strongly suppressed by pressure.

IV. DISCUSSION

From the present studies of ρ on $Ce(Ru_{1-x}Rh_x)_2Al_{10}$ ($x = 0$ and 0.1), we found that although ρ exhibits a Kondo semiconducting increase down to T_0 at the ambient pressure, the increase becomes small with increasing pressure, and then finally disappears at $P \sim 3$ GPa in both samples. Above this pressure, ρ exhibits a broad anomaly at high temperatures, and shows a metallic decrease with decreasing temperature. However, the transition at T_0 persists up to $P_c \sim 4.7$ and 4.5 GPa for $x = 0$ and 0.1, respectively. Also, the transition is clear and T_0 is not so much suppressed by pressure even just below P_c. These results suggest that the hybridization gap could be not necessary to form the unusual AFM order in both samples, $x = 0$ and 0.1. A similar metallic behavior of ρ above T_0 was also observed in $CeOs_2Al_{10}$ near P_c, though the authors did not mention this [31]. A big question here is whether the interaction of the unusual AFM order is a usual indirect exchange interaction mediated by conduction electrons, that is, the RKKY interaction. The suppression of T_0 by a nonmagnetic La substitution clearly indicates that the Ce-4f electrons are necessary to form the AFM order [39]. A critical Ce concentration, $x_c \sim 0.45$, in $(Ce_xLa_{1-x})Ru_2Al_{10}$ suggests that the interaction is long ranged as in the RKKY interaction. However, T_0 is much higher than T_N of GdT_2Al_{10} despite the strong c-f hybridization in CeT_2Al_{10} [40]. Also, the magnetic anisotropy below T_0 is quite unusual; the AFM state with $m_{AF} \parallel c$ or $m_{AF} \parallel b$ is realized despite the strong magnetic anisotropy along the a axis [20]. In addition, the propagation vector in CeT_2Al_{10} is different from those in other LnT_2Al_{10} (Ln = lanthanide) [25,41–43]. Furthermore, the nondivergent behavior of the nuclear spin relaxation rate near T_0 implies no development of spin fluctuations toward T_0 [44]. Thus the interaction of the unusual AFM order could be qualitatively different from the so-called RKKY interaction.

Below $P \sim 3$ GPa, ρ of $CeRu_2Al_{10}$ exhibits a semiconducting upturn at low temperatures. A similar upturn was also observed in $CeOs_2Al_{10}$ and $CeFe_2Al_{10}$ at ambient pressure [6,28,45]. Since the upturn is suppressed by pressure [31,46], the origin of the upturn is ascribed to the c-f hybridization effect. From the results of the optical conductivity, photoemission, and tunneling spectroscopy experiments, there is a fine gap structure inside the hybridization gap [11–14]. There seems to be a certain relation between the low-temperature upturn of ρ and the gap structure. However, at ambient pressure, ρ of $CeRu_2Al_{10}$ exhibits no semiconducting behavior at the lowest temperature, although ρ of $CeOs_2Al_{10}$ shows a clear upturn of ρ at low temperatures [28]. This difference between T = Ru and T = Os could be ascribed to the difference in the electronic structure. The temperature dependence of the Hall coefficient is also different between T = Ru and T = Os [31,47]. Although the low-temperature Hall coefficient is varied by pressure in both T = Ru and T = Os [31,48], it is not so simple to obtain the information on the fine gap formation because the present system is a multicarrier system. Meanwhile, the low-temperature upturn of ρ under pressure is easily suppressed by the Rh doping as shown in

Fig. 3, suggesting that this kind of coherent state is easily broken by the atomic disturbance. However, a similar upturn of ρ is induced by the La, Pr, or Rh doping when the doping level is small [21,49]. At present, we do not know the origin of the low-temperature upturn of ρ in $x = 0$ under pressures. The origin of the upturn of ρ induced by the chemical doping might be different from that induced by pressure. Further systematic studies of the electrical resistivity, Hall effect, and other experiments that can detect the fine gap structure even under pressures are necessary.

Now, let us discuss the pressure dependence of the magnetic susceptibility. χ_a is suppressed by pressure in both samples as shown in Fig. 4. If $\chi_a^{\max}$ decreases continuously with increasing pressure above 2 GPa, $\chi_a^{\max}$ becomes very small near P_c in both samples. In this case, $m_{\rm AF}$ is expected to be also small near $P_{\rm c}$. Assuming the following relation, $T_0 \propto J_{\rm ex} m_{\rm AF}^2$, the exchange integral $J_{\rm ex}$ should be strongly enhanced due to the enhancement of the hybridization effect by pressure in order to achieve the high T_0 near $P_{\rm c}$ as well as the enhancement of T_0 at low pressures especially in $x = 0$. However, it seems to be difficult to explain the nature of the high T_0 by simply a large $J_{\rm ex}$. Based on the Doniach's picture, the AFM transition temperature depends on the c-f hybridization strength. If the hybridization effect is initially weak, the transition temperature is enhanced, and takes a maximum value at a pressure above which the transition temperature is suppressed, and finally goes to zero at $P_{\rm c}$. On the other hand, if the hybridization effect is strong, the transition temperature is simply suppressed, and the AFM ordered state disappears at P_c. Since the hybridization effect is already fairly strong in $CeRu_2Al_{10}$, T_0 is expected to be simply suppressed by pressure especially for $x = 0$ because the hybridization effect is stronger for $x = 0$ than for $x = 0.1$. However, as shown in Fig. 5, T_0 is enhanced by pressure especially for $x = 0$. Also, a mean-field calculation on the magnetic properties has demonstrated that an excessively large $J_{\rm ex}$ gives rise to unrealistic results largely different from the experimental results [50]. Thus it is difficult to explain the nature of the high T_0 by the large $J_{\rm ex}$. Considering the enhancement of T_0 by pressure, a key for the high T_0 could be related to the exchange coupling between the conduction and Ce-4f electrons.

Here we discuss the pressure dependencies of χ_a of $x = 0$ and 0.1 in detail. First, the suppression rate of $\chi_a^{\max}$ by pressure, $d\chi_a^{\max}/dP$, is larger in $x = 0.1$ than in $x = 0$. In $CeOs_2Al_{10}$, $\chi_a^{\max}$ is also linearly suppressed by pressure [31]. Here, $d\chi_a^{\max}/dP$ is smallest in $CeOs_2Al_{10}$, but largest in $Ce(Ru_{0.9}Rh_{0.1})_2Al_{10}$ among them. This indicates that the magnitude of $d\chi_a^{\max}/dP$ is related to the c-f hybridization strength, where it is largest in $CeOs_2Al_{10}$ and smallest in $Ce(Ru_{0.9}Rh_{0.1})_2Al_{10}$. Next, let us discuss the decoupling behavior of T_0 and $T_\chi^{\max}$ in magnetic susceptibility. In usual AF magnets, χ exhibits a maximum at an AFM transition temperature, $T_{\rm N}$, and $T_{\rm N}$ coincides with $T_\chi^{\max}$. In $CeRu_2Al_{10}$, however, T_0 does not coincide with $T_\chi^{\max}$, i.e., $T_0 \sim 27$ K whereas $T_\chi^{\max} \sim 30$ K at the ambient pressure. The difference between T_0 and $T_\chi^{\max}$ becomes pronounced as pressure is applied. This suggests that the origin of the difference is related to the c-f hybridization strength. In $CeOs_2Al_{10}$, the difference is more pronounced than in $CeRu_2Al_{10}$, where $T_0 \sim 29$ K whereas $T_\chi^{\max} \sim 45$ K at ambient pressure. The larger difference in $CeOs_2Al_{10}$ than in $CeRu_2Al_{10}$ is consistent with the fact that the c-f hybridization strength is larger in $CeOs_2Al_{10}$ than in $CeRu_2Al_{10}$. Similar decoupling behavior between $T_\chi^{\max}$ and the AFM transition temperature has been reported in several heavy fermion AF magnets [51]. For instance, in $CeRh_2Si_2$, a sharp cusp of the magnetic susceptibility is observed along the easy magnetization axis, and $T_\chi^{\max}$ coincides with $T_{\rm N}$ at ambient pressure. With increasing pressure, $T_\chi^{\max}$ shifts to high temperatures but $T_{\rm N}$ is monotonically suppressed by pressure [52]. The paramagnetic region between $T_\chi^{\max}$ and $T_{\rm N}$ expands as pressure is applied towards the critical pressure of disappearance of the AFM ordering, and is discussed as a correlated paramagnetic metal (CPM) regime which precursively appears before the AFM ordering [53]. The electronic state in CeT_2Al_{10} above T_0 might be characterized as the CPM regime. On the other hand, by doping a small amount of Rh on $CeRu_2Al_{10}$, T_0 coincides with $T_\chi^{\max}$ even under pressures up to 2.0 GPa at least, and a sharp cusp of χ_a is observed at T_0 as is seen in usual AF magnets. This suggests that the electronic state is qualitatively different between $CeRu_2Al_{10}$ and Rh-doped $CeRu_2Al_{10}$. It is noted that $\chi_a^{\max}$ of $x = 0.1$ at $P \sim 2$ GPa is comparable to that of $x = 0$ at the ambient pressure. This suggests that even if $\chi_a^{\max}$ of $x = 0.1$ becomes as large as that of $x = 0$, the electronic state is qualitatively different between $x = 0$ and 0.1.

From the results of the enhancement of χ_a, and the suppression of the Kondo semiconducting increase of ρ above T_0 as shown in Fig. 1, the c-f hybridization effect must be suppressed by doping the Rh. However, T_0 in $x = 0.1$ is not so much enhanced by pressure as in $x = 0$. Also, $P_{\rm c}$ is rather smaller in $x = 0.1$ than in $x = 0$. These results suggest that the Rh doping does not simply suppress the c-f hybridization effect. Here, the unit-cell volume slightly decreases from 863.6(2) Å in $x = 0$ [54] to 861.3(2) Å in $x = 0.1$. This indicates that the chemical pressure effect is not negative but rather positive. Thus the suppression of the c-f hybridization effect originates not from the lattice expansion, but from the electronic structure change, being related to the anisotropic nature of the c-f hybridization effect. The strong enhancement of χ only along the a axis suggests that the suppression of the hybridization effect is anisotropic. Numerical calculation on the Rh-doped $CeRu_2Al_{10}$ indicates that the electrostatic potential changes anisotropically by the Rh doping [55].

Near $P_{\rm c}$, ρ exhibits no enhancement in the residual resistivity and also in the coefficient A of the T^2 term in ρ. This indicates the lack of quantum fluctuation near $P_{\rm c}$, and thereby the transition at $P_{\rm c}$ could be a first-order transition. From the results of the pressure studies of the lattice parameters and the valence state of Ce ion, it is considered that the origin of $P_{\rm c}$ is neither a structural nor a valence transition [32,33]. Considering the suppression of $\chi_a^{\max}$ toward $P_{\rm c}$, we propose that the origin of $P_{\rm c}$ is related to the disappearance of $m_{\rm AF}$. In the vicinity of $P_{\rm c}$, ρ exhibits a small upturn at low temperatures as shown in the insets of Figs. 2(b) and 3(b). As reported in Ref. [6], a Fermi liquid state is accomplished at much higher pressures. Thus the electronic state just above $P_{\rm c}$ is never a simple metallic Fermi liquid state, representing the basis for the unusual AFM order in CeT_2Al_{10}.

V. CONCLUSIONS

To conclude, we performed the pressure studies of ρ and χ_a on the Kondo semiconductor $Ce(Ru_{1-x}Rh_x)_2Al_{10}$ ($x = 0$ and 0.1) in order to obtain information on the electronic state under pressures, especially what happens near P_c in ρ, and to explore differences between $x = 0$ and 0.1 in pressure responses of ρ and χ_a. From the results of ρ, the critical pressure was determined to be $P_c \sim 4.7$ and 4.5 GPa for $x = 0$ and 0.1, respectively. P_c is nearly the same although the Ce-4f electron state is apparently different between $x = 0$ and 0.1. In both samples, the Kondo-semiconducting behavior of ρ above T_0 was observed up to $P \sim 3$ GPa. Above this pressure, however, ρ exhibits a broad peak at high temperatures, and a metallic decrease with decreasing temperature, and then the AFM order takes place at T_0. This indicates that the hybridization gap could be not necessary to form the unusual AFM order. On the other hand, from the pressure dependence of χ_a, we observed that χ_a is strongly suppressed by pressure in both samples. By increasing the pressure, the broad peak of χ_a in $x = 0$ shifts to high temperatures, whereas the cusp of χ_a for $x = 0.1$ remains sharp and clear up to 2 GPa, suggesting that the electronic states are qualitatively different in $CeRu_2Al_{10}$ and Rh-doped $CeRu_2Al_{10}$. Near P_c, no development of the quantum fluctuation was observed in ρ, suggesting that the transition at P_c could be a first-order transition. Considering the large suppression of $\chi_a^{\max}$ toward P_c by pressure, a possible origin of P_c is the disappearance of m_{AF}.

ACKNOWLEDGMENTS

The authors would like to thank T. Takabatake, Y. Muro, K. Matsubayashi, and A. Kondo for valuable discussions. This work was supported by JSPS KAKENHI Grants No. 26800188, and No. 16K05463.

[1] S. Doniach, Physica B+C (Amsterdam) **91**, 231 (1977).
[2] S. Hoshino and Y. Kuramoto, Phys. Rev. Lett. **111**, 026401 (2013).
[3] G. R. Stewart, Rev. Mod. Phys. **73**, 797 (2001).
[4] P. S. Riseborough, Adv. Phys. **49**, 257 (2000).
[5] A. M. Strydom, Physica B (Amsterdam) **404**, 2981 (2009).
[6] T. Nishioka, Y. Kawamura, T. Takesaka, R. Kobayashi, H. Kato, M. Matsumura, K. Kodama, K. Matsubayashi, and Y. Uwatoko, J. Phys. Soc. Jpn. **78**, 123705 (2009).
[7] Y. Muro, K. Motoya, Y. Saiga, and T. Takabatake, J. Phys. Conf. Ser. **200**, 012136 (2010).
[8] D. D. Khalyavin, A. D. Hillier, D. T. Adroja, A. M. Strydom, P. Manuel, L. C. Chapon, P. Peratheepan, K. Knight, P. Deen, C. Ritter, Y. Muro, and T. Takabatake, Phys. Rev. B **82**, 100405(R) (2010).
[9] H. Tanida, D. Tanaka, Y. Nonaka, M. Sera, M. Matsumura, and T. Nishioka, Phys. Rev. B **84**, 233202 (2011).
[10] H. Kato, R. Kobayashi, T. Takesaka, T. Nishioka, M. Matsumura, K. Kaneko, and N. Metoki, J. Phys. Soc. Jpn. **80**, 073701 (2011).
[11] S. I. Kimura, T. Iizuka, H. Miyazaki, A. Irizawa, Y. Muro, and T. Takabatake, Phys. Rev. lett. **106**, 056404 (2011).
[12] S. I. Kimura, T. Iizuka, H. Miyazaki, T. Hajiri, M. Matsunami, T. Mori, A. Irizawa, Y. Muro, J. Kajino, and T. Takabatake, Phys. Rev. B **84**, 165125 (2011).
[13] T. Ishiga, T. Wakita, R. Yoshida, H. Okazaki, K. Tsubota, M. Sunagawa, K. Uenaka, K. Okada, H. Kumigashira, M. Oshima, K. Yutani, Y. Muro, T. Takabatke, Y. Muraoka, and T. Yokoya, J. Phys. Soc. Jpn. **83**, 094717 (2014).
[14] J. Kawabata, T. Ekino, Y. Yamada, Y. Sakai, A. Sugimoto, Y. Muro, and T. Takabatake, Phys. Rev. B **92**, 201113(R) (2015).
[15] J. Robert, J.-M. Mignot, G. André, T. Nishioka, R. Kobayashi, M. Matsumura, H. Tanida, D. Tanaka, and M. Sera, Phys. Rev. B **82**, 100404(R) (2010).
[16] J. Robert, J.-M. Mignot, S. Petit, P. Steffens, T. Nishioka, R. Kobayashi, M. Matsumura, H. Tanida, D. Tanaka, and M. Sera, Phys. Rev. Lett. **109**, 267208 (2012).
[17] D. T. Adroja, A. D. Hillier, P. P. Deen, A. M. Strydom, Y. Muro, J. Kajino, W. A. Kockelmann, T. Takabatake, V. K. Anand, J. R. Stewart, and J. Taylor, Phys. Rev. B **82**, 104405(R) (2010).
[18] J.-M. Mignot, P. A. Alekseev, J. Robert, S. Petit, T. Nishioka, M. Matsumura, R. Kobayashi, H. Tanida, H. Nohara, and M. Sera, Phys. Rev. B **89**, 161103(R) (2014).
[19] H. Tanida, Y. Nonaka, D. Tanaka, M. Sera, Y. Kawamura, Y. Uwatoko, T. Nishioka, and M. Matsumura, Phys. Rev. B **85**, 205208 (2012).
[20] H. Tanida, D. Tanaka, Y. Nonaka, S. Kobayashi, M. Sera, T. Nishioka, and M. Matsumura, Phys. Rev. B **88**, 045135 (2013).
[21] H. Tanida, H. Nohara, F. Nakagawa, K. Yoshida, M. Sera, and T. Nishioka, Phys. Rev. B **94**, 165137 (2016).
[22] A. Kondo, K. Kindo, K. Kunimori, H. Nohara, H. Tanida, M. Sera, R. Kobayashi, T. Nishioka, and M. Matsumura, J. Phys. Soc. Jpn. **82**, 054709 (2013).
[23] R. Kobayashi, Y. Ogane, D. Hirai, T. Nishioka, M. Matsumura, Y. Kawamura, K. Matsubayashi, Y. Uwatoko, H. Tanida, and M. Sera, J. Phys. Soc. Jpn. **82**, 093702 (2013).
[24] H. Tanida, H. Nohara, M. Sera, T. Nishioka, M. Matsumura, and R. Kobayashi, Phys. Rev. B **90**, 165124 (2014).
[25] R. Kobayashi, K. Kaneko, K. Saito, J.-M. Mignot, G. André, J. Robert, S. Wakimoto, M. Matsuda, S. Chi, Y. Haga, T. D. Matsuda, E. Yamamoto, T. Nishioka, M. Matsumura, H. Tanida, and M. Sera, J. Phys. Soc. Jpn. **83**, 104707 (2014).
[26] S. I. Kimura, H. Tanida, M. Sera, Y. Muro, T. Takabatake, T. Nishioka, M. Matsumura, and R. Kobayashi, Phys. Rev. B **91**, 241120(R) (2015).
[27] D. T. Adroja (unpublished).
[28] J. Kawabata, T. Takabatake, K. Umeo, and Y. Muro, Phys. Rev. B **89**, 094404 (2014).
[29] A. Bhattacharyya, D. T. Adroja, A. M. Strydom, J. Kawabata, T. Takabatake, A. D. Hillier, V. G. Sakai, J. W. Taylor, and R. I. Smith, Phys. Rev. B **90**, 174422 (2014).
[30] D. D. Khalyavin, D. T. Adroja, P. Manuel, J. Kawabata, K. Umeo, T. Takabatake, and A. M. Strydom, Phys. Rev. B **88**, 060403(R) (2013).
[31] K. Umeo, T. Ohsuka, Y. Muro, J. Kajino, and T. Takabatake, J. Phys. Soc. Jpn. **80**, 064709 (2011).
[32] Y. Kawamura, J. Hayashi, T. Keiki, C. Sekine, H. Tanida, M. Sera, and T. Nishioka, J. Phys. Soc. Jpn. **85**, 044601 (2016).

[33] Y. Zekko, Y. Yamamoto, H. Yamaoka, F. Tajima, T. Nishioka, F. Strigari, A. Severing, J.-F. Lin, N. Hiraoka, H. Ishii, K.-D. Tsuei, and J. Mizuki, Phys. Rev. B **89**, 125108 (2014).
[34] H. Tanida, Y. Nonaka, D. Tanaka, M. Sera, T. Nishioka, and M. Matsumura, Phys. Rev. B **86**, 085144 (2012).
[35] K. Kitagawa, H. Gotou, T. Yagi, A. Yamada, T. Matsumoto, Y. Uwatoko, and M. Takigawa, J. Phys. Soc. Jpn. **79**, 024001 (2010).
[36] N. Tateiwa, Y. Haga, Z. Fisk, and Y. Ōnuki, Rev. Sci. Instrum. **82**, 053906 (2011).
[37] N. Tateiwa and Y. Haga, Rev. Sci. Instrum. **80**, 123901 (2009).
[38] T. F. Smith, C. W. Chu, and M. B. Maple, Cryogenics **9**, 53 (1969).
[39] H. Tanida, D. Tanaka, M. Sera, C. Moriyoshi, Y. Kuroiwa, T. Takesaka, T. Nishioka, H. Kato, and M. Matsumura, J. Phys. Soc. Jpn. **79**, 043708 (2010).
[40] M. Sera, H. Nohara, M. Nakamura, H. Tanida, T. Nishioka, and M. Matsumura, Phys. Rev. B **88**, 100404(R) (2013).
[41] M. Reehuis, M. W. Wolff, A. Krimmel, E.-W. Scheidt, N. Stüsser, A. Loidl, and W. Jeitschko, J. Phys.: Condens. Matter **15**, 1773 (2003).
[42] J. Robert, F. Damay, K. Saito, A. M. Bataille, F. Porcher, G. Andre, A. Gukasov, J.-M. Mignot, H. Tanida, and M. Sera, Phys. Rev. B **90**, 224425 (2014).
[43] S. Takai, T. Matsumura, H. Tanida, and M. Sera, Phys. Rev. B **92**, 174427 (2015).
[44] M. Matsumura, N. Tomita, S. Tanimoto, Y. Kawamura, R. Kobayashi, H. Kato, T. Nishioka, H. Tanida, and M. Sera, J. Phys. Soc. Jpn. **82**, 023702 (2013).
[45] Y. Muro, K. Motoya, Y. Saiga, and T. Takabatake, J. Phys. Soc. Jpn. **78**, 083707 (2009).
[46] H. Tanida, M. Nakamura, M. Sera, A. Kondo, K. Kindo, T. Nishioka, and M. Matsumura, J. Phys. Soc. Jpn. **83**, 084708 (2014).
[47] H. Tanida, D. Tanaka, M. Sera, C. Moriyoshi, Y. Kuroiwa, T. Takesaka, T. Nishioka, H. Kato, and M. Matsumura, J. Phys. Soc. Jpn. **79**, 063709 (2010).
[48] Y. Kawamura, Y. Ogane, T. Nishioka, H. Kato, M. Matsumura, D. Tanaka, H. Tanida, M. Sera, A. Kondo, K. Matsubayashi, and Y. Uwatoko, J. Phys. Soc. Jpn. **80**, SA046 (2011).
[49] K. Yoshida, R. Okubo, H. Tanida, T. Matsumura, M. Sera, T. Nishioka, M. Matsumura, C. Moriyoshi, and Y. Kuroiwa, Phys. Rev. B **91**, 235124 (2015).
[50] K. Kunimori, M. Nakamura, H. Nohara, H. Tanida, M. Sera, T. Nishioka, and M. Matsumura, Phys. Rev. B **86**, 245106 (2012).
[51] R. S. T. Takeuchi and Y. Ōnuki, J. Phys. Soc. Jpn. **76**, 051003 (2007).
[52] H. M. N. Takeshita, N. Môri, and Y. Uwatoko, Physica B (Amsterdam) **259-261**, 58 (1999).
[53] W. Knafo, R. Settai, D. Braithwaite, S. Kurahashi, D. Aoki, and J. Flouquet, Phys. Rev. B **95**, 014411 (2017).
[54] M. Sera, D. Tanaka, H. Tanida, C. Moriyoshi, M. Ogawa, Y. Kuroiwa, T. Nishioka, M. Matsumura, J. Kim, N. Tsuji, and M. Takata, J. Phys. Soc. Jpn. **82**, 024603 (2013).
[55] N. Adam, E. Suprayoga, B. Adiperdana, H. Guo, H. Tanida, S. S. Mohd-Tajudin, R. Kobayashi, M. Sera, T. Nishioka, M. Matsumura, S. Sulaiman, M. I. Mohamed-Ibrahim, and I. Watanabe, J. Phys.: Conf. Series **551**, 012053 (2014).